



UNIVERSITY OF LEEDS

This is a repository copy of *Dielectric stability in the relaxor: Na_{0.5}Bi_{0.5}TiO₃-Ba_{0.8}Ca_{0.2}TiO₃-Bi(Mg_{0.5}Ti_{0.5})O₃- NaNbO₃ ceramic system.*

White Rose Research Online URL for this paper:
<http://eprints.whiterose.ac.uk/127274/>

Version: Accepted Version

Article:

Zeb A, and Milne, SJ (2018) Dielectric stability in the relaxor: Na_{0.5}Bi_{0.5}TiO₃-Ba_{0.8}Ca_{0.2}TiO₃-Bi(Mg_{0.5}Ti_{0.5})O₃- NaNbO₃ ceramic system. *Ceramics International*, 44 (7). pp. 7663-7666. ISSN 0272-8842

<https://doi.org/10.1016/j.ceramint.2018.01.191>

© 2018 Elsevier Ltd and Techna Group S.r.l. This manuscript version is made available under the CC-BY-NC-ND 4.0 license <http://creativecommons.org/licenses/by-nc-nd/4.0/>

Reuse

This article is distributed under the terms of the Creative Commons Attribution-NonCommercial-NoDerivs (CC BY-NC-ND) licence. This licence only allows you to download this work and share it with others as long as you credit the authors, but you can't change the article in any way or use it commercially. More information and the full terms of the licence here: <https://creativecommons.org/licenses/>

Takedown

If you consider content in White Rose Research Online to be in breach of UK law, please notify us by emailing eprints@whiterose.ac.uk including the URL of the record and the reason for the withdrawal request.

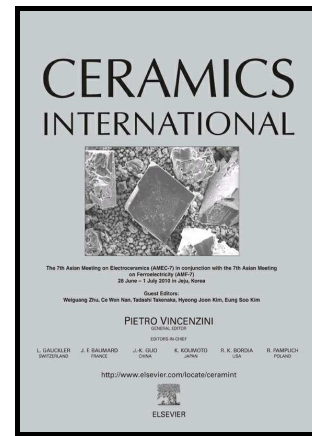


eprints@whiterose.ac.uk
<https://eprints.whiterose.ac.uk/>

Author's Accepted Manuscript

Dielectric stability in the relaxor: $\text{Na}_{0.5}\text{Bi}_{0.5}\text{TiO}_3$ -
 $\text{Ba}_{0.8}\text{Ca}_{0.2}\text{TiO}_3$ - $\text{Bi}(\text{Mg}_{0.5}\text{Ti}_{0.5})\text{O}_3$ - NaNbO_3
ceramic system

Aurang Zeb, Steven J. Milne



PII: S0272-8842(18)30206-2
DOI: <https://doi.org/10.1016/j.ceramint.2018.01.191>
Reference: CER117323

To appear in: *Ceramics International*

Received date: 9 November 2017
Revised date: 18 January 2018
Accepted date: 22 January 2018

Cite this article as: Aurang Zeb and Steven J. Milne, Dielectric stability in the relaxor: $\text{Na}_{0.5}\text{Bi}_{0.5}\text{TiO}_3$ - $\text{Ba}_{0.8}\text{Ca}_{0.2}\text{TiO}_3$ - $\text{Bi}(\text{Mg}_{0.5}\text{Ti}_{0.5})\text{O}_3$ - NaNbO_3 ceramic system, *Ceramics International*, <https://doi.org/10.1016/j.ceramint.2018.01.191>

This is a PDF file of an unedited manuscript that has been accepted for publication. As a service to our customers we are providing this early version of the manuscript. The manuscript will undergo copyediting, typesetting, and review of the resulting galley proof before it is published in its final citable form. Please note that during the production process errors may be discovered which could affect the content, and all legal disclaimers that apply to the journal pertain.

Dielectric stability in the relaxor: $\text{Na}_{0.5}\text{Bi}_{0.5}\text{TiO}_3\text{-Ba}_{0.8}\text{Ca}_{0.2}\text{TiO}_3\text{-Bi}(\text{Mg}_{0.5}\text{Ti}_{0.5})\text{O}_3\text{-NaNbO}_3$ ceramic system

Aurang Zeb^{1,2} and Steven J. Milne¹

¹Institute for Materials Research, University of Leeds, Leeds, LS2 9JT, UK

² Department of Physics, Islamia College Peshawar, KP, Pakistan

*zebicp@gmail.com

Abstract

Ceramics with temperature-stable dielectric characteristics have been developed in the system: $0.6[0.85\text{Na}_{0.5}\text{Bi}_{0.5}\text{TiO}_3\text{-(}0.15\text{-x)}\text{Ba}_{0.8}\text{Ca}_{0.2}\text{TiO}_3\text{-xBi}(\text{Mg}_{0.5}\text{Ti}_{0.5})\text{O}_3]\text{-}0.4\text{NaNbO}_3$, $x \leq 0.15$. Dielectric measurements exhibited relaxor ferroelectric characteristics with temperature-stable relative permittivity from $\epsilon_r \sim 1330 \pm 15\%$ in the temperature range from $-70\text{ }^\circ\text{C}$ – $215\text{ }^\circ\text{C}$ and $\tan\delta \leq 0.02$ from $-20\text{ }^\circ\text{C}$ to $380\text{ }^\circ\text{C}$ for $x = 0$ compositions. For the $\text{Bi}(\text{Mg}_{0.5}\text{Ti}_{0.5})\text{O}_3$ modified compositions the temperature range of stable relative permittivity extended from $-70\text{ }^\circ\text{C}$ to $400\text{ }^\circ\text{C}$, with $\epsilon_r \sim 950 \pm 15\%$ and $\tan\delta \leq 0.02$ from $-70\text{ }^\circ\text{C}$ to $260\text{ }^\circ\text{C}$. Values of dc resistivity were $\sim 10^8\ \Omega\ \text{m}$ at a temperature of $300\text{ }^\circ\text{C}$ and the corresponding RC constant values were in the range from 0.40 - $0.78\ \text{s}$ at $300\text{ }^\circ\text{C}$. All ceramic samples exhibited a linear polarisation-electric field response at maximum applied electric field of $5\ \text{kV/cm}$ ($1\ \text{kHz}$).

Keywords: Temperature stable dielectrics, ceramic capacitors, RC constant

1. Introduction

Stable relative permittivity extending to elevated temperatures $> 200\text{ }^\circ\text{C}$ is of great interest in the search for new types of high volumetric efficiency capacitors for high

temperature environments [1-4]. Conventional barium titanate based high relative permittivity dielectrics are limited to upper working temperatures of ~ 200 °C [5]. A range of ceramics with compositional disorder on A or B cation sites of the ABO_3 perovskite lattice display frequency dependent, broad peaks in the relative permittivity-temperature ϵ_r -T response. These relaxor ferroelectrics have been shown to be a promising starting point from which to achieve a very wide temperature range of stable relative permittivity, with upper limits > 200 °C. This is achieved by engineering increased levels of off-valent lattice substitutions. A plateau-like ϵ_r -T response, giving R-type (± 15 %) stability over wide temperature ranges results [4-11]. Examples include $BaTiO_3$ - $BiMg_{0.5}Ti_{0.5}O_3$ solid solutions which change from ferroelectric to normal relaxor to temperature stable relaxor behaviour with increasing levels of Bi and Mg incorporation [12-15]. Logically this evolution is a result of the decreased coherence length scales between substituent sites on the lattice and consequent interruptions to the length scales of polar order [5].

$Na_{0.5}Bi_{0.5}TiO_3$ (NBT)-based solid solutions have been widely studied for their piezoelectric properties, but also show promising temperature stable relative permittivity characteristics [2, 6, 16]. In some cases the modified NBT-based solid solutions show higher values of relative permittivity than those based on $BaTiO_3$. Xu et al. reported favourable temperature stability in the dielectric system, $Na_{0.5}Bi_{0.5}TiO_3$ - $NaNbO_3$ with a variation in ϵ_r of within $\pm 11\%$ [16]. Dittmer et al. studied the solid solutions; $Na_{0.5}Bi_{0.5}TiO_3$ - $BaTiO_3$ - $K_{0.5}Na_{0.5}NbO_3$ and $Na_{0.5}Bi_{0.5}TiO_3$ - $K_{0.5}Bi_{0.5}TiO_3$ - $K_{0.5}Na_{0.5}NbO_3$, indicating the temperature stable flat plateau of relative permittivity related to size mismatches of the B-site cations [2, 17]. Acosta fabricated the solid solution; $Na_{0.5}Bi_{0.5}TiO_3$ - $BaTiO_3$ - $K_{0.5}Na_{0.5}NbO_3$ by the incorporation of $CaZrO_3$ and reported promising dielectric properties in wide range of temperature -69 to 468 °C. However, the relatively permittivity values were only ~ 500 [6].

In this research article, we report the stability of relative permittivity over a wide temperature range maintaining its value $\sim 900 \pm 15\%$ with low loss tangent for the system: $0.6[0.85\text{Na}_{0.5}\text{Bi}_{0.5}\text{TiO}_3-(0.15-x)\text{Ba}_{0.8}\text{Ca}_{0.2}\text{TiO}_3-x\text{Bi}(\text{Mg}_{0.5}\text{Ti}_{0.5})\text{O}_3]-0.4\text{NaNbO}_3$, $x \leq 0.15$ abbreviated as [NBT-(1-x)BCT-xBMT-NN].

Experimental Procedure

Ceramic samples in the system: $0.6[0.85\text{Na}_{0.5}\text{Bi}_{0.5}\text{TiO}_3-(0.15-x)\text{Ba}_{0.8}\text{Ca}_{0.2}\text{TiO}_3-x\text{Bi}(\text{Mg}_{0.5}\text{Ti}_{0.5})\text{O}_3]-0.4\text{NaNbO}_3$, where x represents the fraction of $\text{Bi}(\text{Mg}_{0.5}\text{Ti}_{0.5})\text{O}_3$ were fabricated by solid state reaction. Four compositions were prepared: $x = 0, 0.05, 0.1, 0.15$. The starting raw powders were: Na_2CO_3 ($\geq 99.5\%$, Sigma Aldrich, St. Louis, MO), Bi_2O_3 (99.9%, Sigma Aldrich), BaCO_3 ($\geq 99\%$ purity; Alpha Aesar, Ward Hill, MA), CaCO_3 ($\geq 99\%$; Sigma Aldrich), MgO (99.9%; Alpha Aesar), Nb_2O_5 (99.9%, Alpha Aesar) and TiO_2 (99.9%, Sigma Aldrich). The raw powders were dried overnight at ~ 200 °C. Appropriate proportions of the powders were ball milled in isopropanol for 24 h. The dried powders were passed through 300 μm nylon mesh sieve and calcined at 850 °C for 3 h at heating and cooling rates of 300 °C/h in a closed alumina crucible. The calcined powders were re-milled again for 24 h after sieving and introducing a binder (Ciba Glascol HA4; Ciba Speciality Chemicals, Bradford UK). After drying and sieving, the powders were uniaxially compacted into disk-shaped pellets in a steel die at ~ 65 MPa followed by cold isostatic pressing at 200 MPa. The pellets (~ 10 mm in diameter and ~ 1.5 mm thickness) were sintered in closed alumina crucibles whilst embedded in an atmosphere powder of the same composition, at 1160 °C for 10 h.

Phase analysis of annealed crushed sintered pellets was performed by using an X-ray diffractometer (XRD Bruker; D8, Karlsruhe, Germany, $\text{Cu-K}\alpha$ $\lambda \sim 1.5406$ Å, scan speed

1°/min) after running the standard. Lattice parameters were deduced by peak profile method using Panalytical HighScore Plus software. For dielectric measurements, the sintered ceramic pellets were ground to ~ 1 mm thickness using 1200 grade silicon carbide papers and silver paste then applied (Agar Scientific, Stansted, UK) and fired at 550 °C for 15 min to form the electrodes. An impedance analyser (HP Agilent, 4192A Hewlett Packard, Santa Clara, CA) was used for relative permittivity ϵ_r and loss tangent ($\tan\delta$) measurement as a function of temperature at different frequencies. Values of dc resistance were recorded as a function of temperature in the range of 250–550 °C using a Keithley 617 programmable electrometer (Cleveland, OH). Polarization-electric field, P-E, response was measured at room temperature using a Precision LC analyser (Radiant Technologies Inc., Albuquerque, New Mexico).

2. Results and discussion

Figure 1 shows room temperature XRD patterns for the annealed crushed sintered pellets of: $0.6[0.85\text{Na}_{0.5}\text{Bi}_{0.5}\text{TiO}_3-(0.15-x)\text{Ba}_{0.8}\text{Ca}_{0.2}\text{TiO}_3-x\text{Bi}(\text{Mg}_{0.5}\text{Ti}_{0.5})\text{O}_3]-0.4\text{NaNbO}_3$, abbreviated as “BMT-modified NBT-BCT-NN ceramics”. Analysis of these patterns revealed a cubic phase with a perovskite structure for all sample compositions but with secondary phases including sodium niobate (ICDD: 04–017–2917) in composition $x = 0.15$, implying a solid solution at $0.1 < x < 0.15$. The a-lattice parameters measured by a peak profile fitting method decreased from $a = 3.91\text{\AA}$ at $x = 0$ to $a = 3.89\text{\AA}$ at $x = 0.15$, Figure 2. There was a low intensity peak ($32.4^\circ 2\theta$) adjacent to the {110} main-phase perovskite peak which corresponds to the most intense reflection in the XRD pattern of NaNbO_3 (ICDD 04-017-2917) indicating incomplete incorporation of NaNbO_3 into the matrix phase.

Plots of ϵ_r -T for all four compositions studied showed characteristics of a relaxor ferroelectric with a suppressed peak, as illustrated in Figure 3. Composition $x = 0$ exhibited a temperature-stable relative permittivity, $\epsilon_r \sim 1330 \pm 15\%$ in the temperature range $-70 - 215$ °C and with low loss $\tan\delta \leq 0.02$ across the temperature-range from -20 °C to 380 °C. The

temperature stable range ($\epsilon_r \pm 15\%$) extends from $-70\text{ }^\circ\text{C}$ to $300\text{ }^\circ\text{C}$ with $\epsilon_r \sim 1240 \pm 15\%$, and $\tan\delta \leq 0.02$ from $-40\text{ }^\circ\text{C}$ to $200\text{ }^\circ\text{C}$ for composition $x = 0.05$. Further incorporation of BMT content in the solid solution extends the temperature stable range from $-70\text{ }^\circ\text{C}$ to $400\text{ }^\circ\text{C}$ and $\tan\delta \leq 0.02$ from $-70\text{ }^\circ\text{C}$ to $260\text{ }^\circ\text{C}$ for composition $x = 0.15$, Table 1. However, at temperatures $> 200\text{ }^\circ\text{C}$ dielectric losses increased and are thought to relate to conductivity arising in part from (mobile) oxygen vacancies and/or electronic conduction relating to oxidation of vacancies, that originate from volatilisation of bismuth oxide during processing [18-20]. This could possibly be minimised by future additions of small excesses of Bi_2O_3 or by alterations to process conditions.

Trends in dielectric properties of the materials studied in this work are presented in Table 1 (1 kHz data).

Values of dc resistivities are plotted versus inverse temperature in Figure 4. There was some variability in the data, but the samples appeared to have high high resistivity. For sample $x = 0$, resistivity, ρ was in the range of $10^9 - 10^8\ \Omega\ \text{m}$ at $250\text{ }^\circ\text{C}$ decreasing to $\sim 10^6\ \Omega\ \text{m}$ at $400\text{ }^\circ\text{C}$. For the other compositions $x \neq 0$, the dc resistivity values were $\sim 10^9 - 10^8\ \Omega\ \text{m}$ at $250\text{ }^\circ\text{C}$ decreasing to $\sim 10^6\ \Omega\ \text{m}$ at $400\text{ }^\circ\text{C}$. These values are comparable to the reported resistivities of other temperature stable relaxor systems [17, 20]. The values of activation energy were, $E_a \sim 0.4-0.5$, in the range normally associated with the migration of oxygen lattice vacancies. There was some evidence of a change in activation energy for conduction as indicated from a change in slope of resistivity plots at a temperature $\geq 400\text{ }^\circ\text{C}$ for $x \neq 0$ compositions [21-23]. Values of RC constant at $300\text{ }^\circ\text{C}$ increased from $0.4\ \text{s}$ for composition $x = 0$ to $0.78\ \text{s}$ for $x = 0.1$, Table 1.

Figure 5 shows polarisation-electric field responses at room temperature. All sample compositions revealed a linear polarisation-electric field response at 50 kV/cm ($f = 1$ Hz) consistent with a low loss capacitor.

In this class of temperature stable relaxor ferroelectric with an extremely diffuse ϵ_r max peak it seems logical to speculate that the suppression of the normal relaxor peak is attributable to the disruption of polar order caused by a high incidence of aliovalent and size mismatched ions. The polarisability and bonding characteristics of Bi, as well as the differences in the displacement characteristics of different A and B site ions are likely to create a highly heterogeneous nano structure, with variability in electrostatic and stress fields over even shorter length scales than in a normal relaxor ferroelectric. This may suppress the increase in coherence length scales on cooling from the Burns temperature that give a strong dielectric peak in a normal relaxor. Hence the normal relaxor dielectric peak becomes progressively inhibited with increasing levels and types of ionic lattice substitutions.. However in highly complex solid solution systems such as NBT-BCT-BMT-NN, microscale chemical heterogeneity may also arise due to incomplete mixing or solid state reaction and so contribute to a very diffuse dielectric response.

3. Conclusions:

Ceramics in the system: $0.6[0.85\text{Na}_{0.5}\text{Bi}_{0.5}\text{TiO}_3-(0.15-x)\text{Ba}_{0.8}\text{Ca}_{0.2}\text{TiO}_3-x\text{Bi}(\text{Mg}_{0.5}\text{Ti}_{0.5})\text{O}_3]-0.4\text{NaNbO}_3$, $x \leq 0.15$ were fabricated by the conventional solid state route. Dielectric data revealed temperature-stable relative permittivities changing by no more than $\pm 15\%$ for temperatures between -70 °C – 300 °C for sample composition $x = 0.1$ and -70 °C to 400 °C for sample composition $x = 0.15$. The dielectric properties of the materials demonstrate the effects of compositional complexity in suppressing the thermal evolution of electric dipoles in perovskite relaxor ferroelectrics. Values of dc resistivity were in the range of $\sim 10^8$ Ω m at 300 °C. Polarisation-electric field responses were linear.

Acknowledgements

A Zeb is thankful to the Higher Education Commission (HEC) Government of Pakistan and Islamia College Peshawar (Chartered University), KP for financial support.

References:

1. J. Watson and G. Castro, A review of high-temperature electronics technology and applications, *J Mater Sci: Mater Electron*, 26; 9226-9235 (2015).
2. R. Dittmer, E.-M. Anton, W. Jo, H. Simons, J. E. Daniels, M. Hoffman, J. Pokorny, I. M. Reaney, and J. Rödel, "A high temperature-Capacitor dielectric Based on $K_{0.5}Na_{0.5}NbO_3$ -Modified $Bi_{1/2}Na_{1/2}TiO_3$ - $Bi_{1/2}K_{1/2}TiO_3$," *J. Am. Ceram. Soc.*, **95** [11]; 3519–24 (2012).
3. N. Raengthon, T. Sebastian, D. Cumming, I. M. Reaney and D. P. Cann, "BaTiO₃-Bi(Zn_{0.5}Ti_{0.5})O₃-BiScO₃ ceramics for high-temperature capacitor applications," *J. Am. Ceram. Soc.*, **95** [11]; 3554-3561 (2012).
4. A. Zeb and S. J. Milne, "High temperature dielectrics ceramics: a review of temperature-stable high-permittivity perovskites," *J Mater Sci: Mater Electron*, 26; 9243-9255 (2015).
5. A. Zeb, Y. Bai, T. Button and S. J. Milne, "Temperature-Stable Relative Permittivity from $-70\text{ }^{\circ}\text{C}$ to $500\text{ }^{\circ}\text{C}$ in $(Ba_{0.8}Ca_{0.2})TiO_3$ - $Bi(Mg_{0.5}Ti_{0.5})O_3$ - $NaNbO_3$ Ceramics" *J. Am. Ceram. Soc.*, 97(8); 2479-2483 (2014).
6. M. Acosta, J. Zang, W. Jo, and J. Rödel, "High-Temperature Dielectrics in $CaZrO_3$ -Modified $Bi_{1/2}Na_{1/2}TiO_3$ -Based Lead-Free Ceramics," *J. Eur. Ceram. Soc.*, 32, 4327–34 (2012).

7. W. Kleemann, "Random Fields in relaxor ferroelectrics-A Jubilee review," *J. advance dielectrics*, 2(2); 1241001(1-13) (2012).
8. A. A. Bokov and Z.-G. Ye, "Recent Progress in Relaxor Ferroelectrics with Perovskite Structure," *J. Mater. Sci.*, **41**[1] 31-52 (2006).
9. V. V. Shvartsman and D. C. Lupascu, "Lead-Free Relaxor Ferroelectrics," *J. Am. Ceram. Soc.*, **95** [1]; 1–26 (2012).
10. T. Wang, L. Jin, C. Li, Q. Hu, and X. Wei, Relaxor Ferroelectric BaTiO₃–Bi(Mg_{2/3}Nb_{1/3})O₃ Ceramics for Energy Storage Application, *J. Am. Ceram. Soc.*, **98** [2]; 559–566 (2015).
11. A. Zeb and S.J . Milne, "High temperature dielectrics in the ceramic system K_{0.5}Bi_{0.5}TiO₃-Ba(Zr_{0.2}Ti_{0.8})O₃-Bi(Zn_{2/3}Nb_{1/3})O₃, " *Ceramic International*, **43**, 7724-7727 (2017).
12. Q. Zhang, Z. Li, F. Li, Z. Xu, "Structural and Dielectric Properties of BaTiO₃–Bi(Mg_{0.5}Ti_{0.5})O₃ Lead-Free Ceramics," *J. Am. Ceram. Soc.*, **94**[12]: 4335–39 (2011).
13. B. Xiong, H. Hao, S. Zhang, H. Liu, and M. Cao, "Structure, dielectric properties and temperature stability of BaTiO₃–Bi (Mg_{1/2}Ti_{1/2})O₃ perovskite solid solutions" *J. Am. Ceram. Soc.*, **94**, 3412–3417(2011).
14. D. H Choi, A. Baker, M. Lanagan, S. Trolier-McKinstry and C. Randall, "Structural and Dielectric Properties in (1-x)BaTiO₃-xBi(Mg_{1/2}Ti_{1/2})O₃ Ceramics (0.1≤ x ≤0.5) and Potential for High-Voltage Multilayer Capacitors," *J. Am. Ceram. Soc.*, **96**[7], 2197-2202 (2013).
15. A. Zeb and S. J. Milne, Stability of High-Temperature Dielectric Properties for (1-x) Ba_{0.8}Ca_{0.2}TiO₃-xBi(Mg_{0.5}Ti_{0.5})O₃ Ceramics, *J. Am. Ceram. Soc.* **96**, 2887-2892 (2013).

16. Q. Xu, Z. Song, W. Tang, H. Hao, L. Zhang, M. Appiah, M. Cao, Z. Yao, Z. He and H. Liu “Ultra-Wide Temperature Stable Dielectrics Based on $\text{Bi}_{0.5}\text{Na}_{0.5}\text{TiO}_3\text{--NaNbO}_3$ System” *J. Am. Ceram. Soc.*, **98** [10] 3119–3126 (2015).
17. R. Dittmer, W. Jo, D. Damjanovic, and J. Rödel, “Lead-free high-temperature dielectrics with wide operational range,” *J. Appl. Phys.*, **109**, 034107 (1-5)(2011).
18. T. Bongkarn, G Rujijanagul, S. J. Milne “Effect of Excess PbO on Phase Formation and Properties of $(\text{Pb}_{0.9}\text{Ba}_{0.1})\text{ZrO}_3$ ” *Mats. Letts.* 59[10]; 1200-1205 (2005).
19. W. Ge, J. Li and D. Viehland “Influence of Mn Doping on the Structure and Properties of $\text{Na}_{0.5}\text{Bi}_{0.5}\text{TiO}_3$ Single Crystals” *J. Am. Ceram. Soc.* 93 [5], 1372-1377 (2010).
20. A. Zeb and S.J Milne, Temperature-stable dielectric properties from $-20\text{ }^\circ\text{C}$ to $430\text{ }^\circ\text{C}$ in the system $\text{BaTiO}_3\text{--Bi}(\text{Mg}_{0.5}\text{Zr}_{0.5})\text{O}_3$, *J. Eur. Ceram. Soc.*, **34**, 3159-3166 (2014).
21. R. Selvamani, G. Singh, V.S. Tiwari, P. K. Gupta, “Oxygen vacancy related relaxation and conduction behaviour in $(1-x)\text{NBT--xBiCrO}_3$ solid solution. *Phys. Status Solid A*, **209**:118–25.34 (2012).
22. F. D. Morrison, D. C. Sinclair, A.R. West. Electrical and structural characteristics of lanthanum-doped barium titanate ceramics. *J. Appl. Phys.*, **86**:6355–66 (1999).
23. A. Zeb and S.J Milne, Low variation in relative permittivity over the temperature range $25\text{--}450\text{ }^\circ\text{C}$ for ceramics in the system $(1-x)[\text{Ba}_{0.8}\text{Ca}_{0.2}\text{TiO}_3]\text{--}x[\text{Bi}(\text{Zn}_{0.5}\text{Ti}_{0.5})\text{O}_3]$, *J. Eur. Ceram. Soc.*, **34**, 1727-1732 (2014).

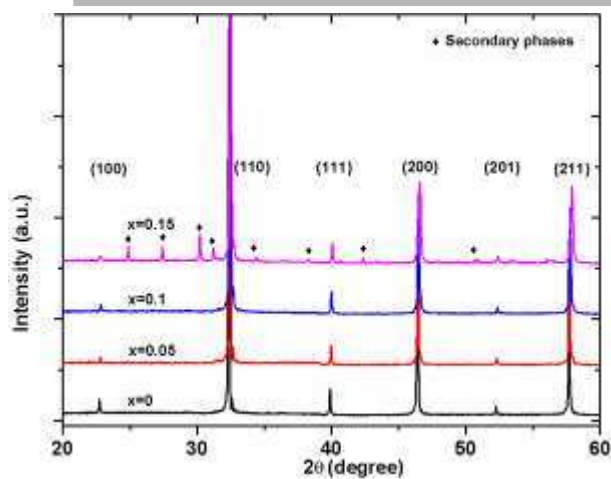


Figure 1. Room temperature XRD patterns for crushed sintered pellets for ceramics in the system: NBT-(1-x)BCT-xBMT-NN, $x \leq 0.15$.

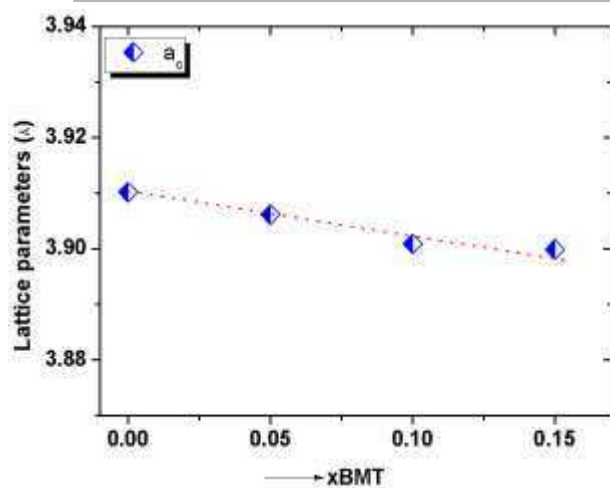


Figure 2. Room temperature lattice parameters as a function of xBMT.

Accepted manuscript

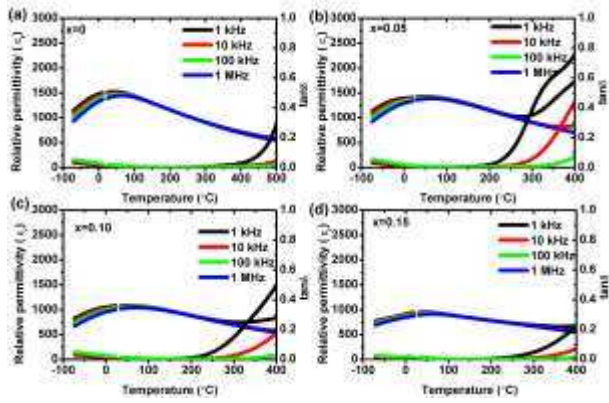


Figure 3. Temperature dependence of relative permittivity and $\tan\delta$ at various frequencies for the system: NBT-(1-x)BCT-xBMT-NN, $x \leq 0.15$. (a) $x = 0$, (b) $x = 0.05$, (c) $x = 0.10$ and (d) $x = 0.15$ (break shows the switching of low to high temperature instruments).

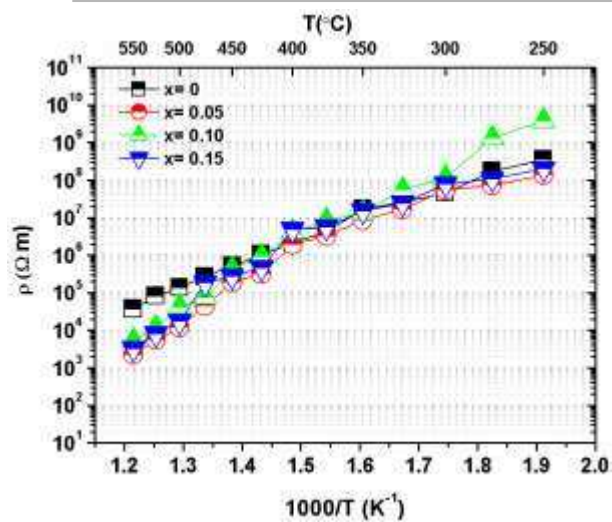


Figure 4. Variation of dc resistivity as a function of $1/T$ (absolute temperature) for the system: $\text{NBT}-(1-x)\text{BCT}-x\text{BMT}-\text{NN}$, $x \leq 0.15$.

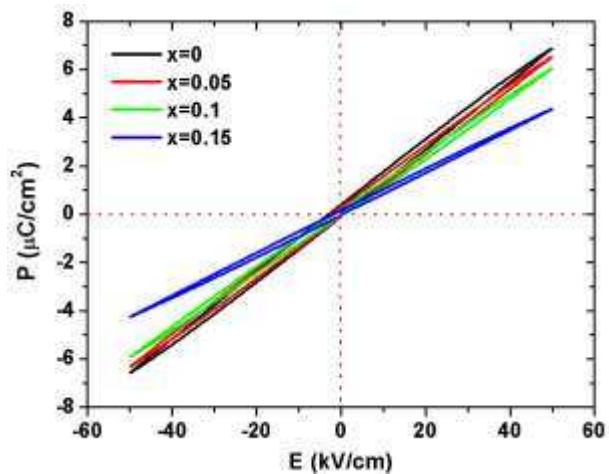


Figure 5. Polarisation-Electric field responses at 50 kV/cm for xBMT content in the system: NBT-(1-x)BCT-xBMT-NN, $x \leq 0.15$.

Accepted manuscript

Table 1. Summary of the dielectric properties of: NBT-(1-x)BCT-xBMT-NN, $x \leq 0.15$; ϵ_r and $\tan\delta$ values, resistivities and RC constants measured at 1 kHz.

Measured parameters	$x = 0$	$x = 0.05$	$x = 0.10$	$x = 0.15$
T_m (°C)	30	50	30	20
ϵ_r max	1530	1430	1080	950
T-range (°C)	“-70 to +215”	“-70 to +300”	“-70 to +250”	“-70 to +400”
$\epsilon_r \pm 15\%$	(1330)	(1240)	(940)	(830)
T-range (°C) $\tan\delta \leq 0.02$	“-20 to +380”	“-40 to +200”	“-30 to +220”	“-70 to +260”
Resistivity (Ω m), 300 °C	4.6×10^7	1.3×10^8	1.2×10^8	6.0×10^8
RC constant (s), 300 °C	0.40	0.52	0.78	0.49